

# Factors That Govern the Performance of Thermal Interface Materials

PARISA POUR SHAHID SAEED ABADI,<sup>1</sup> CHIA-KEN LEONG,<sup>1</sup>  
and D.D.L. CHUNG<sup>1,2</sup>

1.—Composite Materials Research Laboratory, University at Buffalo, State University of New York, Buffalo, NY 14260-4400, USA. 2.—e-mail: ddlchung@buffalo.edu

Finite element modeling is conducted to understand the factors that govern the performance of thermal interface pastes of controlled thickness between copper surfaces of controlled roughness. Carbon black paste is lower in thickness than metal particle paste, so it shows better performance. The performance of both pastes is more influenced by the paste-copper interfacial conductance than by the paste thermal conductivity. The effects of pressure, paste thickness, and copper surface roughness on performance are mainly due to the change in fractional filling of the valleys in the copper surface topography. Reasonable agreement is found between modeling and experimental results.

**Key words:** Thermal interface material, thermal paste, thermal contact conductance, thermal conductivity, finite element modeling, carbon black

## INTRODUCTION

A thermal interface material (TIM) refers to a material that is placed at the interface between two surfaces that are at different temperatures in order to improve the heat transfer between the surfaces.<sup>1,2</sup> The improvement of the thermal contact between a microprocessor and a heat sink (or a heat spreader) of a computer is particularly important, since heat dissipation is the most critical problem in the microelectronic industry. Due to the technological need, the development of TIMs has resulted in numerous products on the market. However, evaluation and understanding of the performance of the interface materials have not kept up with the market boom, though they are essential for the advancement of this field.

A TIM typically comprises a paste, which is called a thermal paste. The paste may be the entire thermal interface material, or it may be a part of the TIM. In the latter case, the paste typically coats

both sides of a thin carrier sheet (e.g., a metal foil), which facilitates handling and use of the TIM.

The performance of a TIM should be evaluated when the TIM is sandwiched between selected surfaces, rather than being evaluated when the interface material is standing alone. The latter gives the thermal conductivity of the TIM itself; although this thermal conductivity is a factor affecting performance, it does not describe the performance of the material as a thermal interface material.

The sandwich mentioned above is a system that consists of the TIM and the two interfaces between the interface material and the two proximate surfaces. Each of these two interfaces is associated with a thermal resistance (referred to as the interfacial resistance), which can contribute significantly to the overall thermal resistance of the sandwich. The interfacial resistance depends on the nature of the interface as well as on the area of this interface. This area is the true interface area that takes into account the area of the interface associated with the filled part of a valley in the surface topography. The true interface area increases with fractional filling of the valleys. This is to be distinguished from the macroscopic geometric area of the thermal interface.

(Received July 4, 2007; accepted September 8, 2008;  
published online October 10, 2008)

The performance of a TIM depends on the structure of the interface between the TIM and each of the two surfaces, in addition to depending on the structure and thickness of the TIM. The structure of the interface depends on the surface roughness (particularly the typical height and width of the valleys in the topography of the surface) and the fractional filling of the valleys. The thickness of the TIM is often referred to as the bond-line thickness. The fractional filling of the valleys depends on the roughness of the surface, the pressure applied in the direction perpendicular to the interface for the purpose of squeezing the proximate surfaces together, and the elastic modulus, viscosity, and conformability of the TIM. A low modulus and a low viscosity help the spreadability. The higher the modulus, the greater the pressure required for the TIM to flow. In practical microelectronic applications, the pressure is limited. A low modulus and a low viscosity also help the conformability, but conformability requires not just the ability to flow macroscopically, but the ability to fill microscopic valleys (even those on the nanoscale) in the surface topography. The filling of the valleys is necessary in order to displace the air, which is thermally insulating, from the valleys. For the purpose of filling microscopic valleys, a microscopically structured (preferably nanostructured) interface material is valuable. An example of a nanostructured TIM is a carbon black thermal paste, in which the carbon black particles are 30 nm in size.<sup>3–11</sup> Another example is a carbon nanotube thermal paste,<sup>12,13</sup> though it is inferior in performance to the carbon black paste. Yet another example is a carbon nanotube array coating,<sup>14–17</sup> which is also inferior to the carbon black paste. Commercial thermal pastes tend to be microstructured rather than nanostructured.

The relative importance of the various parameters mentioned above depends on the combination of values of the various parameters. For example, the thermal conductivity of the TIM becomes more important as the thickness of the TIM increases and as the surface roughness (i.e., the height of the valleys in the surface topography) increases; the interfacial conductance (i.e., the reciprocal of the interfacial resistivity, which is the product of the interfacial resistance and the true interface area, with the interface referring to that between the TIM and one of the surfaces) becomes more important as the true interface area decreases.

The performance of a TIM is described by the thermal contact conductance (TCC, in units of  $W/m^2 K$ ), which refers to the thermal conductance of the overall thermal contact in the direction perpendicular to the plane of the sandwich. This conductance is the reciprocal of the thermal contact resistivity (in units of  $m^2 K/W$ ), which is the product of the total thermal resistance (in units of  $K/W$ , i.e., the temperature difference across the thermal contact divided by the heat power) of the thermal

contact and the geometric area (in units of  $m^2$ ) of the thermal interface. Due to the number and interdependence of the various parameters mentioned above in governing TCC, a complete experimental investigation of all the parameters is difficult. Furthermore, it is difficult to obtain TIMs that cover a substantial range of each of the parameters (including the thermal conductivity, modulus, viscosity, and conformability) for the purpose of a systematic experimental evaluation. Therefore, understanding of the performance of TIMs requires modeling of this performance. This modeling is the objective of this paper.

Prior work on modeling TIM performance has involved analytical models. Most commonly, the modeling is based on an equivalent circuit of the thermal resistance, which includes those of the TIM and of the interface between the TIM and each of the two proximate surfaces.<sup>2,18–21</sup> The thermal resistance of this interface has been modeled by consideration of the degree of filling of the valleys in the surface topography.<sup>2,18,19</sup> However, the complexity of the combination of geometric, thermal, mechanical, and material factors calls for finite element modeling, which is the method used in this work. The use of simple analytical equations in place of finite element modeling was found in this work to be inadequate, so no analytical model is presented here.

The performance of a TIM depends on a number of parameters, especially the surface roughness, TIM thickness, TIM thermal conductivity, TIM modulus, interfacial conductance of the copper-TIM (Cu-TIM) interface, interfacial conductance of the copper-copper (Cu-Cu) interface, and applied pressure. Prior experimental work<sup>3–10,12</sup> addressed specific thermal interface materials without covering a substantial range of any parameter. The objective of the modeling work of this paper is to evaluate systematically the effect of each of these parameters. Furthermore, the relative importance of these various factors is addressed for two contrasting thermal pastes—one being highly conformable (carbon black paste) and the other being high in thermal conductivity (metal particle paste manufactured by Shin-Etsu).

In order to test the validity of the model, the modeling results of this work are compared with experimental results on carbon black paste (polyethylene glycol vehicle with 1.25 vol.% carbon black) and a metal particle paste (widely used commercial Shin-Etsu X-23-7762 paste, which is aluminum-particle-filled silicone with a density of 2.6 g/ml, manufactured by Shin-Etsu MicroSi, Inc., Phoenix, AZ). Due to the high solid content in the metal particle paste compared with the carbon black paste, the metal particle paste is much higher in modulus and thickness. However, the metal particle paste is much more thermally conductive than the carbon black paste. Due to the large difference in properties between the two pastes, comparison of

the modeling results for the two pastes is expected to help understand the factors that govern the performance of a thermal paste.

### MODELING METHODOLOGY

The finite element modeling was conducted using commercial ANSYS software. The modeling was two dimensional. It was assumed that no heat loss to the environment occurs. In accordance with the experimental condition of TCC measurement by the guarded hot-plate method,<sup>3-5</sup> the TIM is sandwiched by two copper blocks of specified roughness.

The surface roughness is modeled as consisting of a semicircle, such that the semicircles of the two proximate surfaces are aligned, with the bottom of a semicircular hillock of the upper surface aligned with the top of a semicircular hillock of the lower surface, as illustrated in Fig. 1. The dimensions and boundary temperatures in Fig. 1 are shown in Table I. This model considers only the bottom portion of the upper copper block and the top portion of the lower copper block. These hillock shapes are used because they roughly represent the actual situation and are similar to the hemispherical hillocks used in three-dimensional contact models in prior analytical work.<sup>22,23</sup> Because displacement in the horizontal direction is negligible, a symmetric boundary condition can be applied on vertical lines that bound the copper blocks and the TIM (Fig. 1). Therefore, this model with one hillock roughly represents the actual case with a large number of hillocks. For the proof of accuracy, for one case, the results of this model were compared with another model with more hillocks; no considerable change was observed when increasing the number of hillocks.

The dimensions shown in Fig. 1 were used in the modeling. The carbon black TIM thickness was  $0.4 \mu\text{m}$  in the rough case and  $0.16 \mu\text{m}$  to  $0.24 \mu\text{m}$  in the smooth case, based on experimental values.<sup>3-5</sup> The metal particle TIM thickness was  $2.9 \mu\text{m}$  to  $4.0 \mu\text{m}$  in the rough case and  $2.6 \mu\text{m}$  to  $3.4 \mu\text{m}$  in the smooth case, based on experimental values.<sup>3-5</sup> This large difference between the two pastes is due to the much higher viscosity of the metal particle paste. During the formation of the thermal contact, the TIM enters the valleys to a degree that depends on the combination of pressure and TIM modulus.

All stages before applying pressure cannot be modeled because of the limited information available on the nonlinear behavior of the pastes. So, either the final geometry after applying pressure is modeled (as for the rough and smooth cases for the carbon black TIM, and the smooth case for the metal particle TIM) or the initial TIM thickness and TIM modulus are selected based on the final (i.e., after pressure application) experimental values (as for the smooth case for the metal particle TIM). Figures 2 and 3 show the initial geometries for the rough and smooth cases, respectively. In fact, only

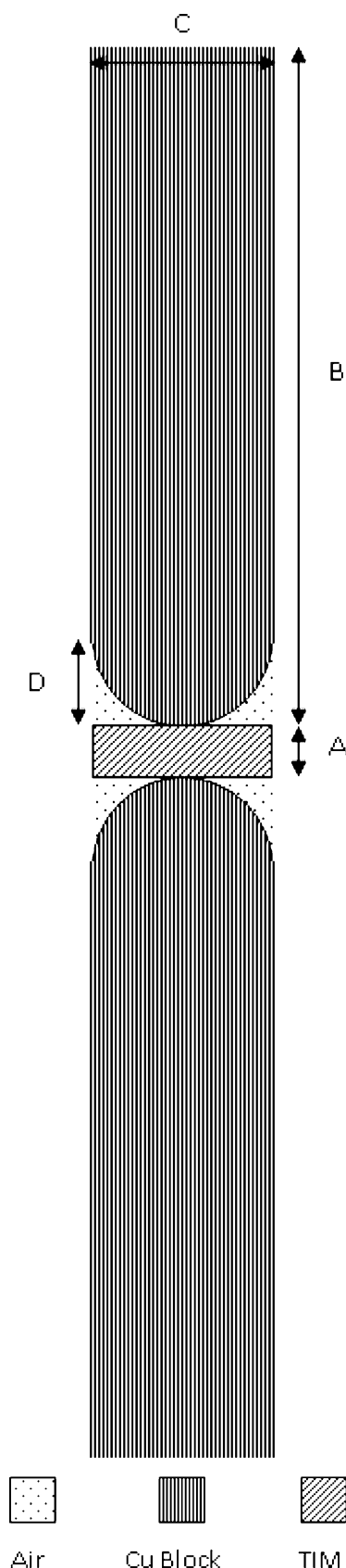


Fig. 1. Initial state (before any pressure is applied) of the thermal contact structure used in the modeling, unless noted otherwise. The dimensions indicated in Table I are used.

Table I. Dimensions in Fig. 1

TIM	Roughness	A ( $\mu\text{m}$ )	B ( $\mu\text{m}$ )	C ( $\mu\text{m}$ )	D ( $\mu\text{m}$ )	$T_t$ ( $^{\circ}\text{C}$ )	$T_b$ ( $^{\circ}\text{C}$ )
Carbon black	Rough	0.4	150	30	15	35.66	34.68
Carbon black	Smooth	0.2	150	30	0.01	35.66	34.68
Metal particle	Rough	3.5	150	30	15	35.66	34.68
Metal particle	Smooth	2.9	150	30	0.01	35.66	34.68

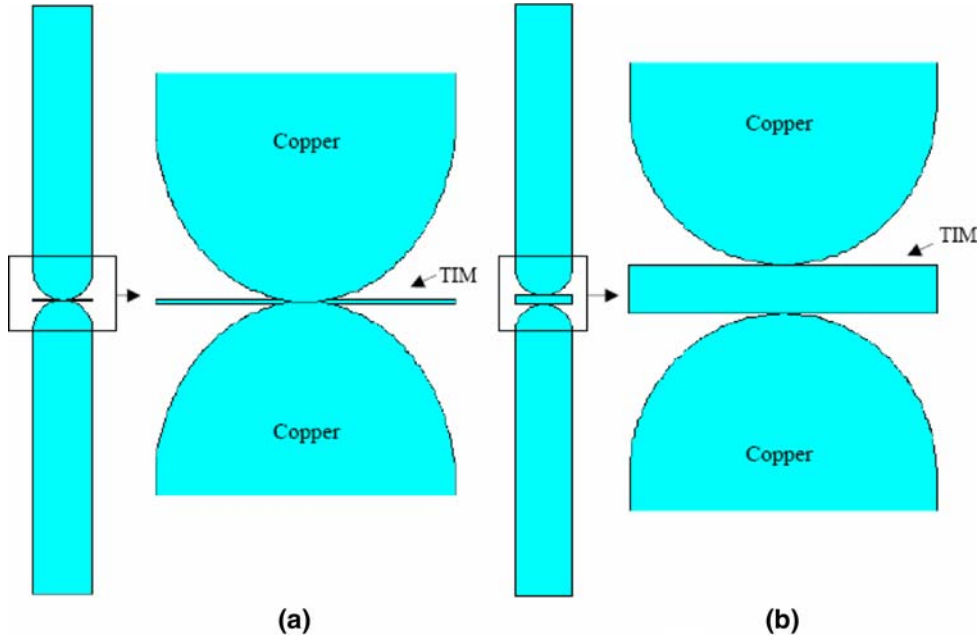


Fig. 2. Initial state of the models for the rough case. (a) Carbon black paste. (b) Metal particle paste.

the final geometry, which is predicted (based on experimental results on the bond line thickness<sup>3-5</sup>) and modeled, affects the calculated thermal contact conductance. Previous stages, before this final state, do not affect the final results.

In the case of rough copper surfaces and the carbon black TIM, no change of bond-line thickness was experimentally observed<sup>5</sup> with increasing pressure in the range of 0.46 MPa to 0.92 MPa. However, the measured TCC increased with increasing pressure in this case.<sup>3-5</sup> Based on these experimental results on the effect of pressure, we assume in this modeling that direct contact between the copper blocks and blunting (plastic deformation) of the copper hillocks occur. With increasing pressure, more blunting occurs, thus increasing the contact area of the two copper surfaces and causing the TCC to increase.

The initial conditions specified in the model are the thickness of the TIM, the temperature ( $T_b$  in Fig. 1) at the bottom surface of the modeled top portion of the lower copper block, and the temperature ( $T_t$  in Fig. 1) at the top surface of the modeled

bottom portion of the upper copper block. The temperature  $T_t$  is calculated from the temperature gradient (0.093 $^{\circ}\text{C}/\text{mm}$ , as in the experiment<sup>3</sup>) and  $T_b$ . However, according to the definition of the thermal contact conductance (the heat flux divided by the temperature difference across the thermal contact), the results are independent of the selected values of  $T_b$  and  $T_t$ . This independence is because both the temperature difference across the thermal contact and the heat power similarly depend on the difference between  $T_b$  and  $T_t$ , so that the quotient is independent of this quantity.

The sides of the geometry in Fig. 1 are assumed to be thermally insulated. Thermal expansion is ignored. The mechanical boundary condition is such that the bottom block is fixed in position. Upon the application of pressure in the direction perpendicular to the thermal contact, a part of the TIM enters the valleys and eventually achieves a steady state (final state), which is the state described by the results reported here.

The extent of filling of a valley can be calculated from the valley geometry and half of the

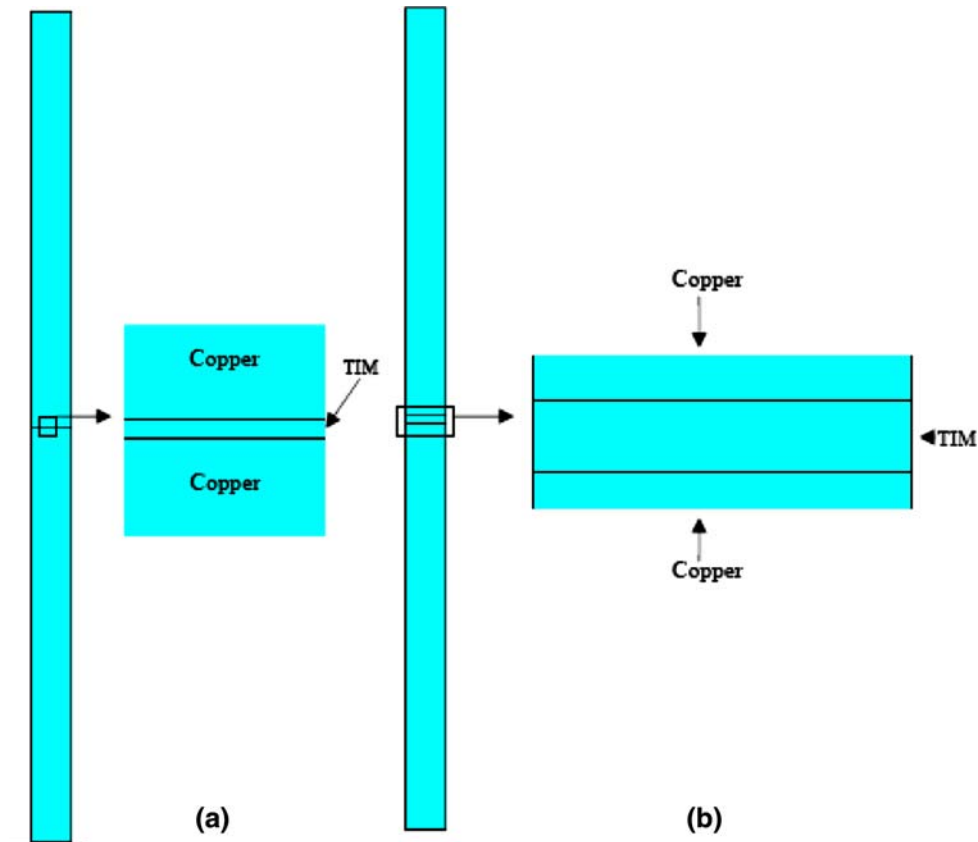


Fig. 3. Initial state of the models for the smooth case. (a) Carbon black paste. (b) Metal particle paste.

displacement of the proximate copper surfaces relative to one another. The factor of half is due to the fact that filling occurs at the valleys of both copper blocks simultaneously. The displacement here is the entire displacement of one copper block relative to the other.

The finite element mesh is shown in Figs. 4 and 5 for the case of rough and smooth copper surfaces,

respectively. The meshes for both the carbon black paste and the metal particle paste are shown in each figure. The ANSYS elements PLANE223 (two-dimensional eight-node coupled-field solids), CONTA172 (two-dimensional three-node surface-to-surface contact), and TARGE169 (two-dimensional target segment) are used. The elements near the contact area are particularly small.

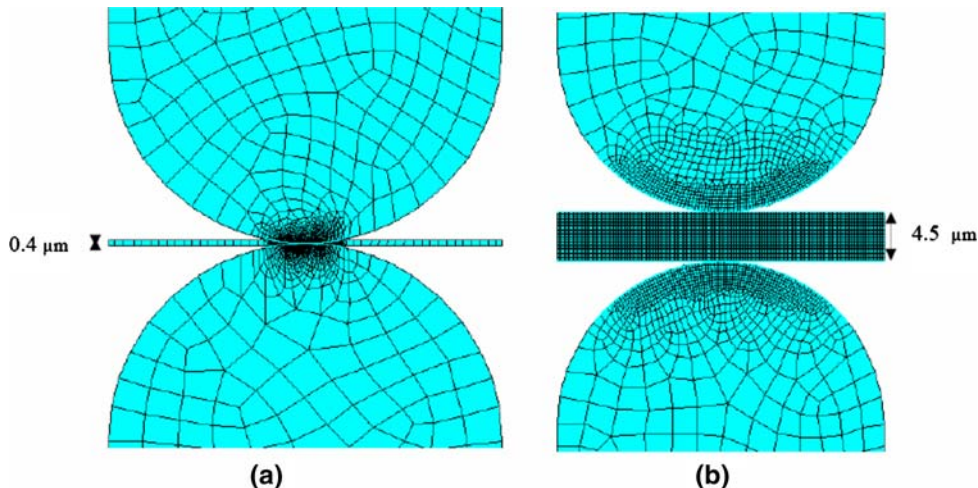


Fig. 4. Finite element mesh for the models shown in Fig. 2.

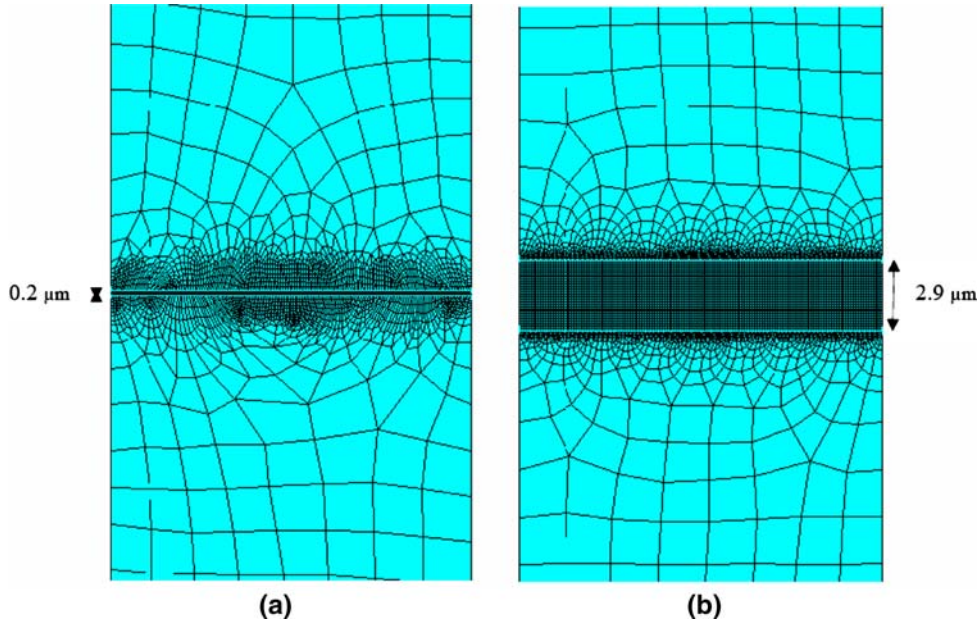


Fig. 5. Finite element mesh for the models shown in Fig. 3.

In calculating the temperature distribution by FEM, the following equations are used.

$$q = kA \frac{dT}{dx}, \quad (1)$$

where  $q$  is the (one-dimensional) heat flow per unit time across the cross-sectional area  $A$ ,  $k$  is the thermal conductivity of the medium, which is copper, air or TIM, depending on the location;  $k$  is not a variable in the modeling work.  $T$  is the temperature;  $x$  is the distance in the direction of heat flow from the top surface of the upper copper block.

$$Q = \frac{q}{A} = k \frac{dT}{dx}, \quad (2)$$

where  $Q$  is the heat flux. The heat diffusion equation is

$$\frac{\partial}{\partial x} \left( k \frac{\partial T}{\partial x} \right) + \frac{\partial}{\partial y} \left( k \frac{\partial T}{\partial y} \right) + \frac{\partial}{\partial z} \left( k \frac{\partial T}{\partial z} \right) + \dot{q} = \rho C_p \frac{\partial T}{\partial t}, \quad (3)$$

where  $x$ ,  $y$ , and  $z$  are the coordinates,  $\rho$  is the density,  $C_p$  is the specific heat, and  $\dot{q}$  is the rate of energy generation per unit volume ( $\text{W/m}^3$ ). Under steady-state conditions, there is no change in the amount of energy and Eq. 3 reduces to

$$\frac{\partial}{\partial x} \left( k \frac{\partial T}{\partial x} \right) + \frac{\partial}{\partial y} \left( k \frac{\partial T}{\partial y} \right) + \frac{\partial}{\partial z} \left( k \frac{\partial T}{\partial z} \right) + \dot{q} = 0. \quad (4)$$

For the case of one-dimensional heat flow in the absence of heat generation, Eq. 4 becomes

$$\frac{d}{dx} \left( k \frac{dT}{dx} \right) = 0. \quad (5)$$

The two-dimensional temperature distribution is obtained by calculation at each of the nodes in the finite element mesh. The mesh is much finer near the thermal contact than in the region further away from it. The temperature drop across the thickness of the TIM is obtained from the two-dimensional temperature distribution and is used to calculate the TCC.

The modulus and pressure are two parameters that greatly affect the thermal contact conductance. This is mainly because of their effects on the extent of filling of the valleys in the surface topography. It can also be due to their effects on the extent of blunting of the hillocks in the surface topography. A lower modulus and a higher pressure will result in more filling of the valleys and, in some cases, also more blunting of the hillocks, thereby leading to a higher thermal contact conductance. Furthermore, a higher pressure can result in a lower TIM thickness. In the modeling work, the modulus and pressure influence the outcome by affecting the dimensions.

The unfilled portion of each valley is filled with air, which is taken to have a thermal conductivity in the range from 0.026 W/m K to 0.028 W/m K.<sup>24</sup> The thermal conductivity of air (0.026 W/m K to 0.028 W/m K)<sup>24</sup> is low compared with that of the TIM (0.13 W/m K to 6 W/m K).<sup>3,4</sup> Therefore, the areas which are in contact with air can be assumed to be thermally insulating, as is done in this

modeling. The thermal conductivity of copper is 391 W/m K.<sup>20</sup> The modulus of copper is 115 GPa.<sup>20</sup>

Both the thermal conductivity and the thickness are much higher for the metal particle paste than the carbon black paste. The difference is mainly because of the much higher solid content of the metal particle paste than the carbon black paste.

In studying the effect of the TIM thermal conductivity by modeling, the conductivity is varied from 0.078 W/m K to 7 W/m K; this range is consistent with the calculated value of 0.128 W/m K for carbon black paste<sup>4</sup> and 6 W/m K for the metal particle paste.<sup>3</sup>

In studying the effect of the roughness height (i.e., initial hillock height) by modeling, this height is varied from 0.01  $\mu\text{m}$  to 15  $\mu\text{m}$ ; this range is consistent with the roughness of 0.009  $\mu\text{m}$  and 15  $\mu\text{m}$  used in the experiment.<sup>3</sup>

In studying the effect of pressure by modeling, the pressure is varied from 0.46 MPa to 0.92 MPa; this range is consistent with the values of 0.46 MPa, 0.69 MPa, and 0.92 MPa used in the experiment.<sup>3</sup>

In studying the effect of the interfacial conductance, the Cu-TIM interfacial conductance is varied from  $50 \times 10^4 \text{ W/m}^2 \text{ K}$  to  $110 \times 10^4 \text{ W/m}^2 \text{ K}$  and the Cu-Cu interfacial conductance is varied from  $60 \times 10^6 \text{ W/m}^2 \text{ K}$  to  $80 \times 10^6 \text{ W/m}^2 \text{ K}$ ; these ranges are selected so that the resulting TCCs are close to the experimental values. The fact that, for both rough and smooth cases, the calculated TCCs are close to experimental values for these ranges of interfacial conductance shows the accuracy of the selected range for the Cu-TIM interfacial conductance. The Cu-Cu interfacial conductance affects only the results of the rough case of the carbon black TIM, because of contact between the copper blocks in this case. As a result of the very low roughness of the copper blocks in the smooth case with either paste as the TIM, and the high thickness and high modulus in the rough case with the metal particle paste as the TIM, there is no contact between the copper blocks and the Cu-Cu interfacial conductance has no effect on the results in these cases. There is no prior report of relevant interfacial conductance values.

The experimental results used in this work for comparison with the modeling results were obtained in prior work<sup>3,4</sup> using the method described below. The TCC between two 1 in  $\times$  1 in (25 mm  $\times$  25 mm) copper blocks with a thermal interface material between them was measured using the guarded hot-plate method, which is a steady-state method of heat flux measurement (ASTM method D5470). During the period of temperature rise, the heating rate was controlled at 3.2°C/min by using a temperature controller. Heating was provided by heating coils, while cooling was provided by running water. The two mating surfaces of the two 1 in  $\times$  1 in copper blocks were either “rough”

(15  $\mu\text{m}$  roughness, as attained by mechanical polishing) or “smooth” (0.009  $\mu\text{m}$  roughness and 0.040  $\mu\text{m}$  to 0.116  $\mu\text{m}$  flatness, as attained by diamond turning). Four thermocouples (type T) were inserted into four holes ( $T_1$ ,  $T_2$ ,  $T_3$ , and  $T_4$  in Fig. 6, each hole of diameter 2.4 mm). Two of the four holes were located in each of the 1 in  $\times$  1 in copper blocks. The temperature gradient was determined from  $T_1 - T_2$  and  $T_3 - T_4$ . These two quantities should be equal at equilibrium, which was attained after holding the temperature of the heater at the desired value for 30 min. Equilibrium was assumed when the temperature variation was within  $\pm 0.1^\circ\text{C}$  in a period of 15 min. The pressure in the direction perpendicular to the plane of the thermal interface was controlled by using a hydraulic press at pressures of 0.46 MPa, 0.69 MPa, and 0.92 MPa.

In accordance with ASTM method D5470, the heat flow  $q$  is given by

$$q = \frac{kA}{d_A} \Delta T, \quad (6)$$

where  $\Delta T = T_1 - T_2 = T_3 - T_4$ ,  $k$  is the thermal conductivity of copper,  $A$  is the area of the 1 in  $\times$  1 in copper block, and  $d_A$  is the distance between thermocouples  $T_1$  and  $T_2$  (i.e., 25 mm).

The temperature at the top surface of the thermal interface material is  $T_A$ , which is given by

$$T_A = T_2 - \frac{d_B}{d_A} (T_1 - T_2), \quad (7)$$

where  $d_B$  is the distance between thermocouple  $T_2$  and the top surface of the thermal interface material (i.e., 5 mm). The temperature at the bottom surface of the thermal interface material is  $T_D$ , which is given by

$$T_D = T_3 + \frac{d_D}{d_C} (T_3 - T_4), \quad (8)$$

where  $d_D$  is the distance between thermocouple  $T_3$  and the bottom surface of the thermal interface material (i.e., 5 mm) and  $d_C$  is the distance between thermocouples  $T_3$  and  $T_4$  (i.e., 25 mm). The thermal resistivity  $\theta$  is given by

$$\theta = (T_A - T_D) \frac{A}{q}. \quad (9)$$

Note that insertion of Eq. 6 into Eq. 9 causes cancellation of the term  $A$ , so that  $\theta$  is independent of  $A$ . The thermal contact conductance is the reciprocal of  $\theta$ .

## MODELING RESULTS

The modeling results are presented below for both carbon black paste and metal particle paste. For either paste, the two-dimensional temperature distributions are presented. In addition, for each

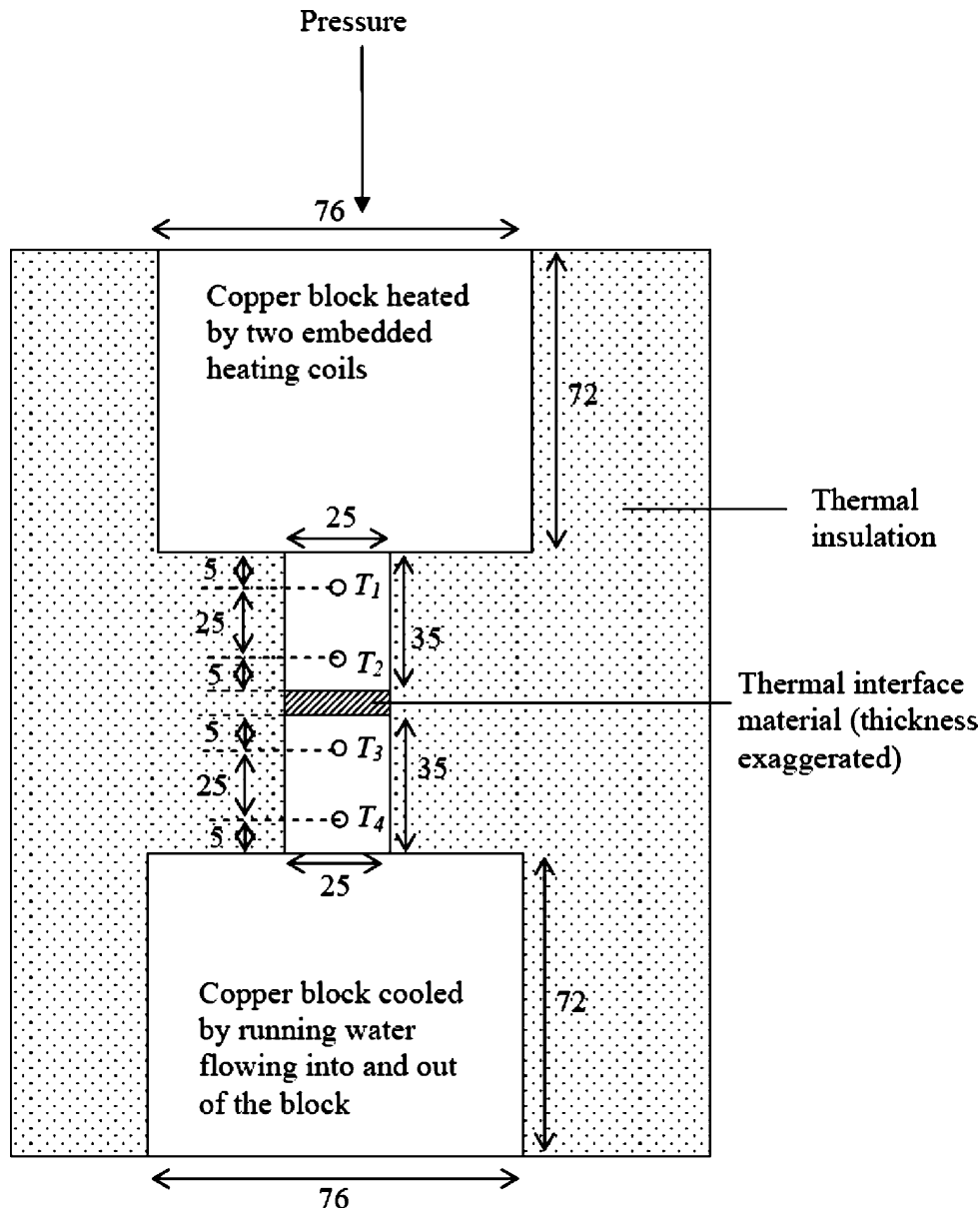


Fig. 6. Experimental setup for the guarded hot-plate method of thermal contact conductance measurement.  $T_1$ ,  $T_2$ ,  $T_3$ , and  $T_4$  are the temperatures at the holes of diameter 2.4 mm. A thermocouple (type T) is inserted in each hole. All dimensions are in millimeters.

paste, the effects of the various parameters on the calculated thermal contact conductance (TCC) and the fractional valley filling are presented. These parameters include the pressure, interfacial conductance (conductance of the interface between the TIM and copper for the part where the TIM and copper are in direct contact and between copper and copper for the part where two copper hillocks are in direct contact), TIM thermal conductivity, TIM thickness, and copper roughness (i.e., hillock height). Furthermore, the calculated TCCs for both carbon black paste and metal particle paste, each evaluated for both rough and smooth cases, are compared with the corresponding experimental results.

### Two-Dimensional Temperature Distribution from Modeling

This section gives the two-dimensional temperature distributions for carbon black and metal particle pastes. For each case, the parameters used reflect the experimental conditions. The effect of the choice of parameters is addressed in the section "Effects of Various Parameters on the Calculated Thermal Contact Conductance."

#### Carbon Black Paste

*Case of rough copper surfaces:* Figure 7 shows the two-dimensional temperature distribution for the case of rough copper blocks when the carbon

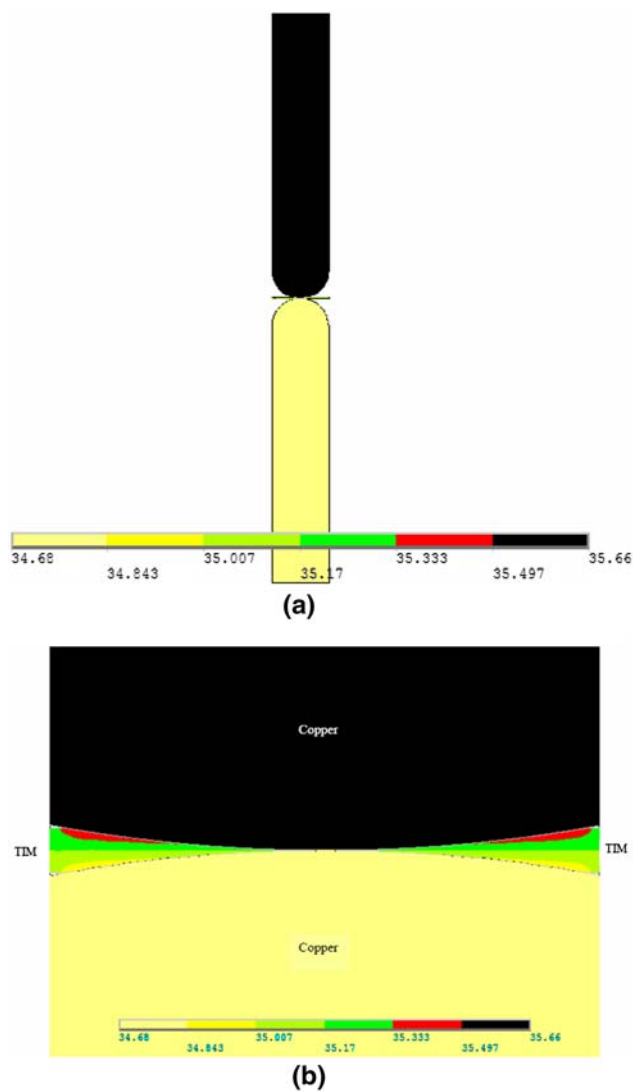


Fig. 7. Finite element modeling result (the deformed state of the model), showing the two-dimensional temperature distribution for the rough case with the carbon black paste as the TIM. (a) Full view. (b) Expanded view of the region in the vicinity of the thermal contact.

black paste is the TIM. The model parameters (as chosen to fit the experimental data) were: pressure = 0.69 MPa, TIM thermal conductivity = 0.13 W/m K, Cu-TIM interfacial conductance (i.e., the reciprocal of the thermal resistivity of the interface between TIM and copper) =  $105 \times 10^4$  W/m<sup>2</sup> K, Cu-Cu interfacial conductance =  $7 \times 10^7$  W/m<sup>2</sup> K, copper roughness (i.e., hillock height) = 15  $\mu$ m, and TIM thickness = 0.4  $\mu$ m.

*Case of smooth copper surfaces:* Figure 8 shows the two-dimensional temperature distribution for the case of smooth copper blocks when the carbon black paste is the TIM. The model parameters (as chosen to fit the experimental data) were: pressure = 0.69 MPa, TIM thermal conductivity = 0.13 W/m K, Cu-TIM interfacial conductance (i.e., the reciprocal

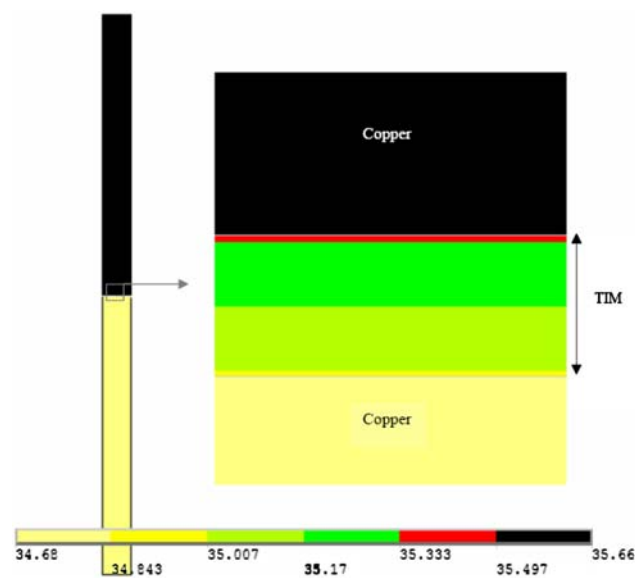


Fig. 8. Finite element modeling result (the deformed state of the model), showing the two-dimensional temperature distribution for the smooth case with the carbon black paste as the TIM.

of the thermal resistivity of the interface between TIM and copper) =  $105 \times 10^4$  W/m<sup>2</sup> K, copper roughness (i.e., hillock height) = 0.01  $\mu$ m, and TIM thickness = 0.2  $\mu$ m.

### Metal Particle Paste

*Case of rough copper surfaces:* Figure 9 shows the two-dimensional temperature distribution for the case of rough copper blocks when the metal particle paste is the TIM. The model parameters were: pressure = 0.69 MPa, TIM thermal conductivity = 6 W/m K, interfacial conductance =  $50 \times 10^4$  W/m<sup>2</sup> K, copper roughness = 15  $\mu$ m, and TIM thickness = 3.5  $\mu$ m.

*Case of smooth copper surfaces:* Figure 10 shows the two-dimensional temperature distribution for the case of smooth copper blocks when the metal particle paste is the TIM. The model parameters were: pressure = 0.69 MPa, TIM thermal conductivity = 6 W/m K, interfacial conductance =  $50 \times 10^4$  W/m<sup>2</sup> K, copper roughness = 0.01  $\mu$ m, and TIM thickness = 2.9  $\mu$ m.

### Effects of Various Parameters on the Calculated Thermal Contact Conductance

#### Carbon Black Paste

*Case of rough copper surfaces:* The effects of (i) the interfacial conductance between the TIM and copper (for the part in which the TIM and copper are in direct contact), (ii) the interfacial conductance between copper and copper (for the part in which the two copper hillocks are in direct contact), (iii) TIM thermal conductivity, (iv) copper surface

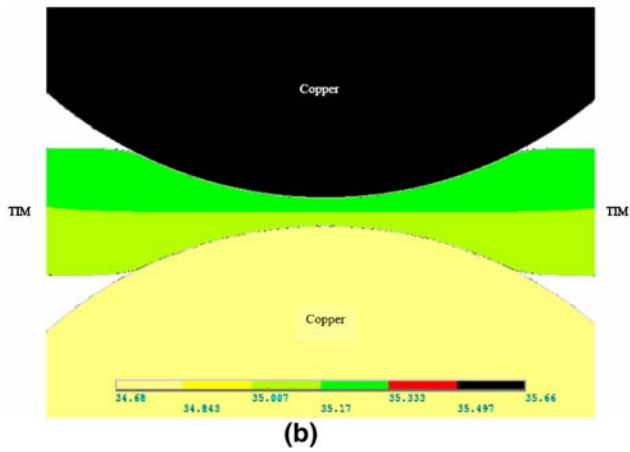
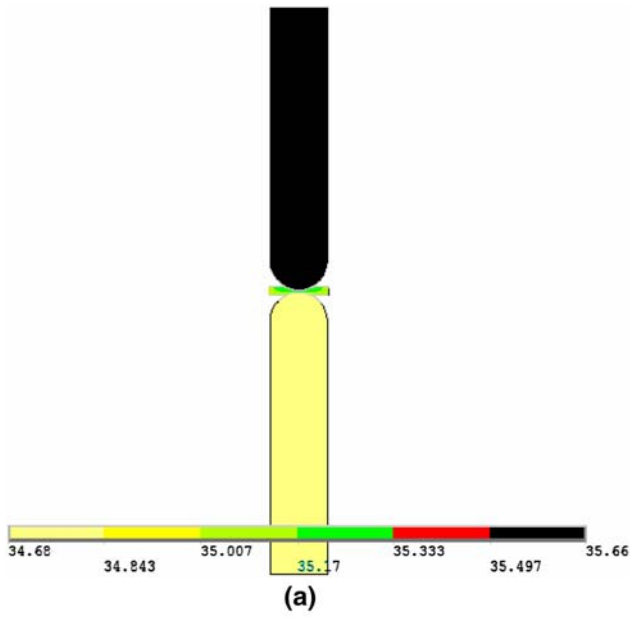


Fig. 9. Finite element modeling result (the deformed state of the model), showing the two-dimensional temperature distribution for the rough case with the metal particle paste as the TIM. (a) Full view. (b) Expanded view of the region in the vicinity of the thermal contact.

roughness (initial valley height, which is the same as the initial hillock height), (v) TIM thickness, and (vi) pressure on the thermal contact conductance (TCC) for the carbon black paste (case of rough copper blocks) are shown in Figs. 11–16, respectively. The fractional valley filling, as calculated based on the modeling result, is shown in Figs. 14 and 15, in order to help explain the TCC trends.

The combination of parameters is such that the TCC obtained by the modeling is in line with experimental values.<sup>3,4</sup> The TCC increases with increasing TIM-Cu and Cu-Cu interfacial conductances (Figs. 11 and 12). This effect is greater for the Cu-TIM interfacial conductance than for the Cu-Cu interfacial conductance because the contact area between copper and the TIM is much larger than that between copper and copper. The TCC increases with increasing TIM thermal conductivity (Fig. 13),

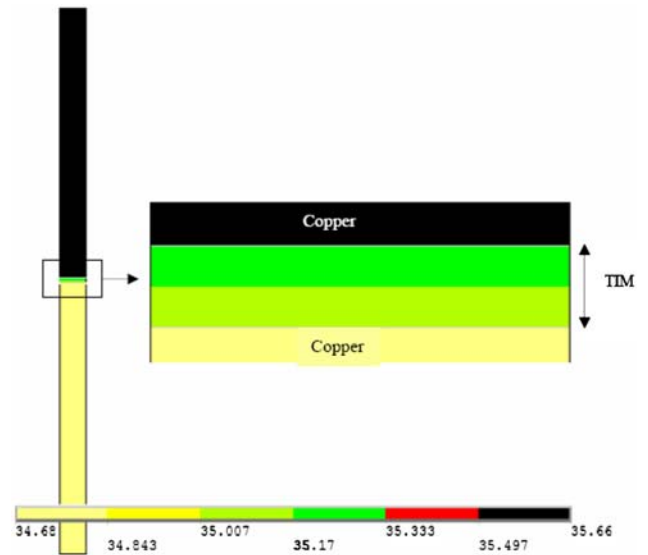


Fig. 10. Finite element modeling result (the deformed state of the model), showing the two-dimensional temperature distribution for the smooth case with the metal particle paste as the TIM.

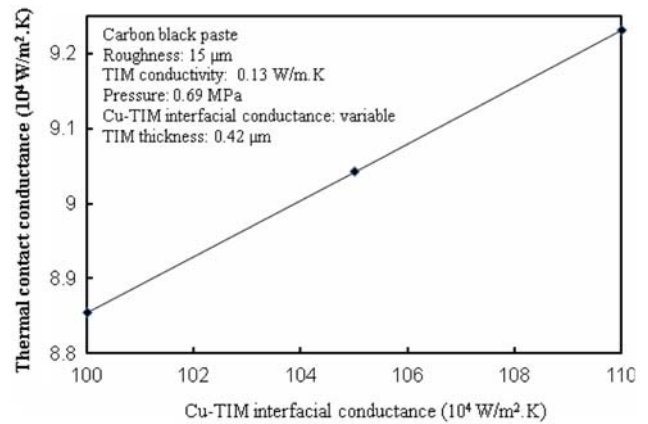


Fig. 11. Effect of the TIM-copper interfacial conductance on the thermal contact conductance for the carbon black paste as the TIM (the rough case).

with decreasing roughness (Fig. 14), with decreasing TIM thickness (Fig. 15), and with increasing pressure (Fig. 16). The fact that the TCC increases with decreasing roughness is because of the associated increase in the fractional final valley filling and larger contact area between copper and the TIM. The fact that TCC increases with decreasing initial TIM thickness is a result of the shorter heat flow path and/or the direct contact between two copper surfaces. In relation to the dependence of TCC on the TIM thickness, the abrupt decrease in TCC in the low-thickness regime of Fig. 15 is presumably because of the presence of direct contact between the copper surfaces when the TIM thickness is relatively low. This assumption of direct contact between copper surfaces is supported by experimental results,<sup>3–5</sup> as explained in the “Modeling Methodology” section.

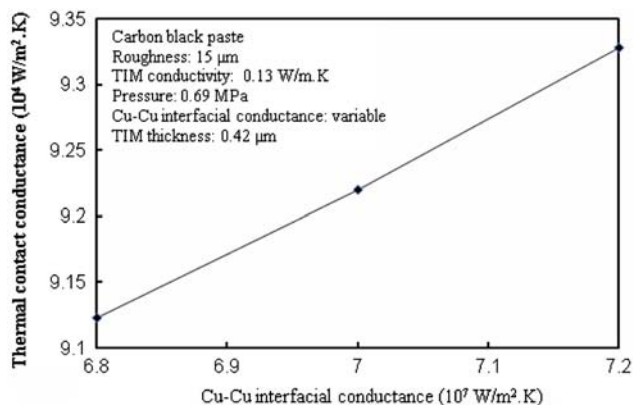


Fig. 12. Effect of the copper-copper interfacial conductance on the thermal contact conductance for the carbon black paste as the TIM (the rough case).

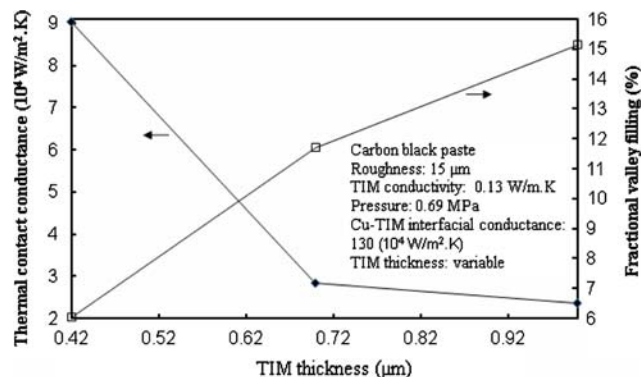


Fig. 15. Effect of the TIM thickness on the thermal contact conductance and on the fractional final valley filling for the carbon black paste as the TIM (the rough case).

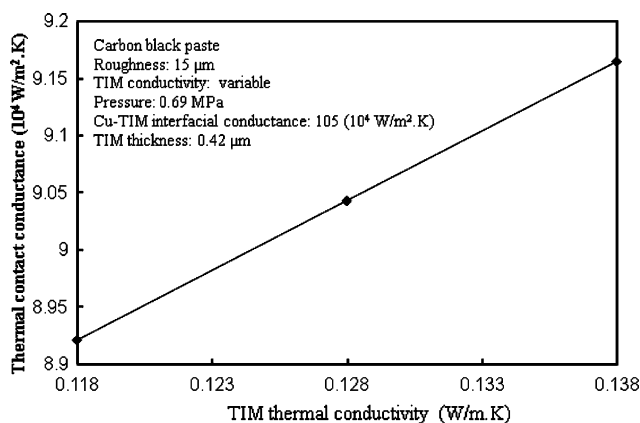


Fig. 13. Effect of the TIM thermal conductivity on the thermal contact conductance for the carbon black paste as the TIM (the rough case).

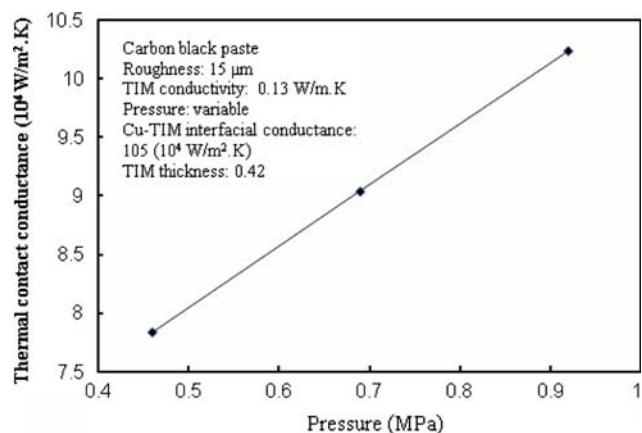


Fig. 16. Effect of pressure on the thermal contact conductance for the carbon black paste as the TIM (the rough case).

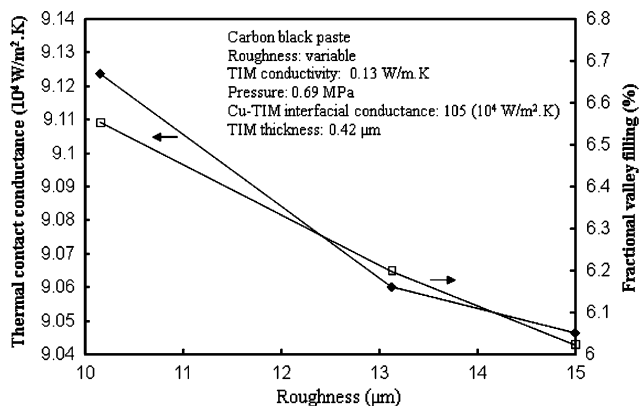


Fig. 14. Effect of roughness (i.e., hillock height) on the thermal contact conductance and on the fractional final valley filling for the carbon black paste as the TIM (the rough case).

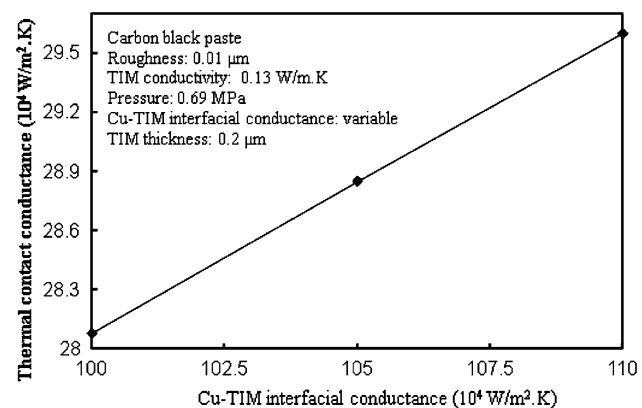


Fig. 17. Effect of the TIM-copper interfacial conductance on the thermal contact conductance for the carbon black paste as the TIM (the smooth case).

*Case of smooth copper surfaces:* The effects of (i) the copper-TIM interfacial conductance, (ii) the TIM thermal conductivity, (iii) the TIM thickness, and (iv) the pressure on the TCC for the carbon black paste (case of smooth copper blocks) are shown in Figs. 17–20, respectively. The combination of

parameters is such that the TCC obtained by the modeling is in line with experimental values.<sup>3,4</sup> The TCC increases with increasing copper-TIM interfacial conductance (Fig. 17), with TIM thermal conductivity (Fig. 18), with decreasing TIM thickness (Fig. 19), and with increasing pressure (Fig. 20). Fractional valley filling in the smooth case

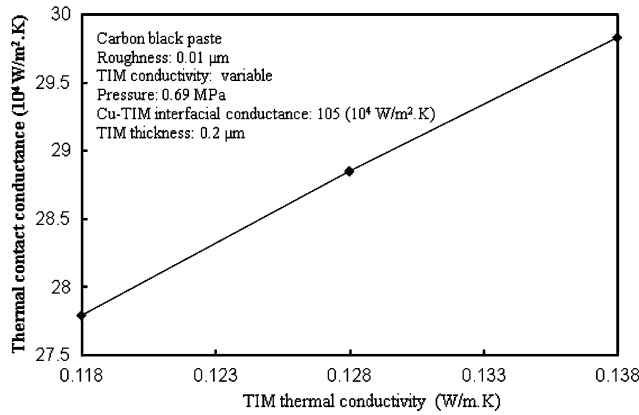


Fig. 18. Effect of the TIM thermal conductivity on the thermal contact conductance for the carbon black paste as the TIM (the smooth case).

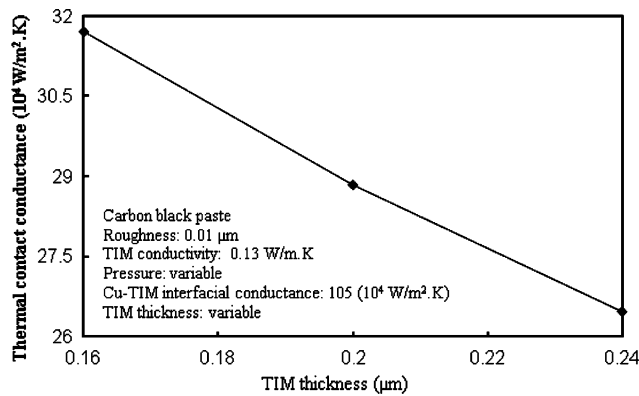


Fig. 19. Effect of the TIM thickness on the thermal contact conductance for the carbon black paste as the TIM (the smooth case).

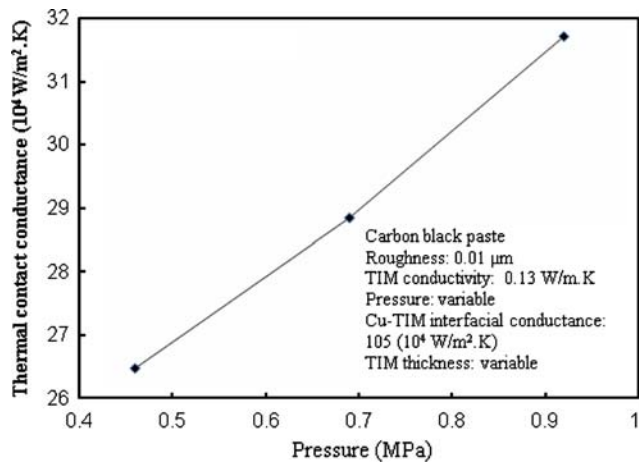


Fig. 20. Effect of pressure on the thermal contact conductance for the carbon black paste as the TIM (the smooth case).

is 100%. Increasing pressure (decreasing thickness) decreases the length of the heat flow path, thereby increasing the TCC.

*Metal Particle Paste*

*Case of rough copper surfaces:* The effects of (i) the interfacial conductance, (ii) the TIM thermal

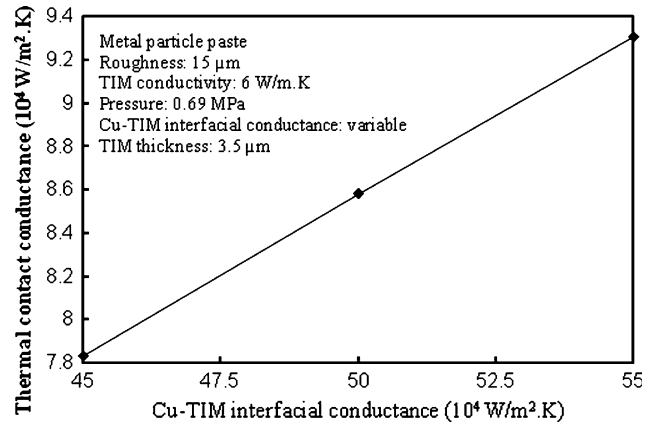


Fig. 21. Effect of the TIM-copper interfacial conductance on the thermal contact conductance for the metal particle paste as the TIM (the rough case).

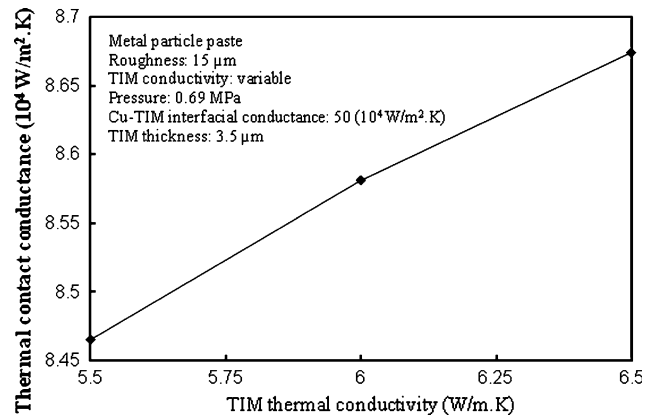


Fig. 22. Effect of the TIM thermal conductivity on the thermal contact conductance for the metal particle paste as the TIM (the rough case).

conductivity, (iii) the copper surface roughness (initial hillock height), (iv) the TIM thickness, and (v) the pressure on the TCC for the metal particle paste (case of rough copper blocks) are shown in Figs. 21–25, respectively. The fractional valley filling, as calculated based on the modeling result, is shown in Figs. 23–25.

The effects of the interfacial conductance, TIM thermal conductivity, and roughness on the TCC are similar to these effects for the carbon black paste (see the section “Case of Rough Copper Surfaces”). Figure 24 shows a different trend of the effect of TIM thickness for the metal particle paste compared with that for the carbon black paste (Fig. 15). The fact that TCC increases with increasing thickness in Fig. 24 is because increasing the metal particle paste thickness increases both the heat flow path and the fractional valley filling, as shown in Fig. 24. In this range of thickness, the positive effect of increasing the fractional valley filling is dominant and causes the TCC to increase. With a more significant increase in thickness, the other factor (i.e., the longer heat flow path) becomes dominant, thus causing the TCC to decrease with

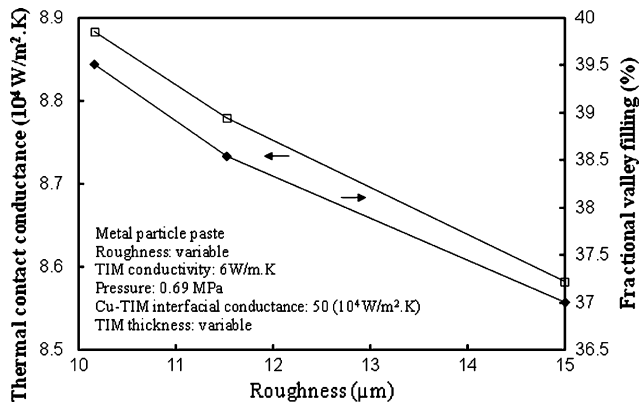


Fig. 23. Effect of the roughness (i.e., hillock height) on the thermal contact conductance and on the fractional final valley filling for the metal particle paste as the TIM (the rough case).

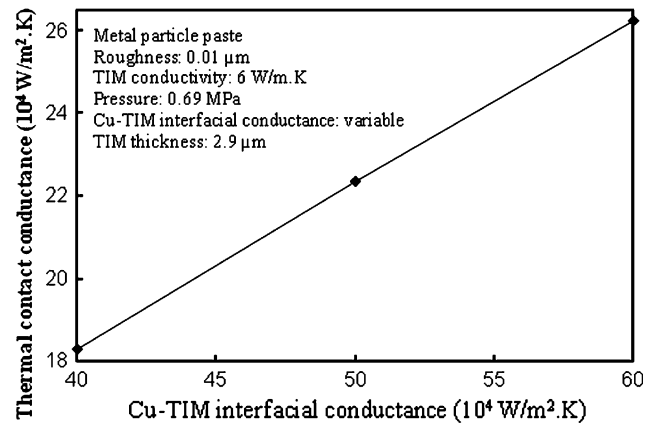


Fig. 26. Effect of the TIM-copper interfacial conductance on the thermal contact conductance for the metal particle paste as the TIM (the smooth case).

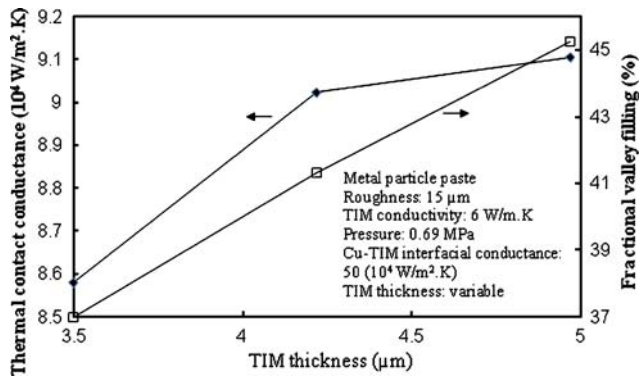


Fig. 24. Effect of the TIM thickness on the thermal contact conductance and on the fractional final valley filling for the metal particle paste as the TIM (the rough case).

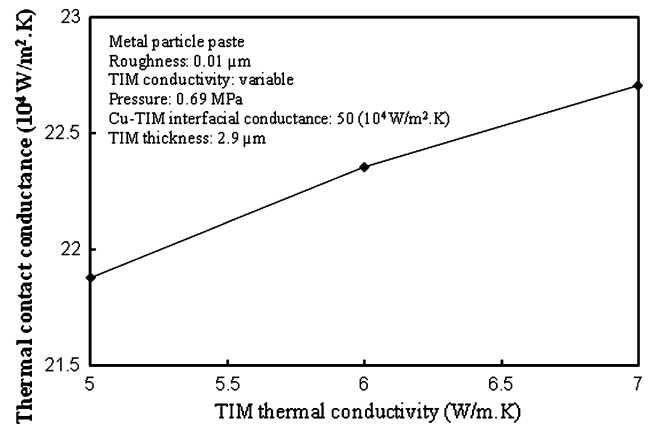


Fig. 27. Effect of the TIM thermal conductivity on the thermal contact conductance for the metal particle paste as the TIM (the smooth case).

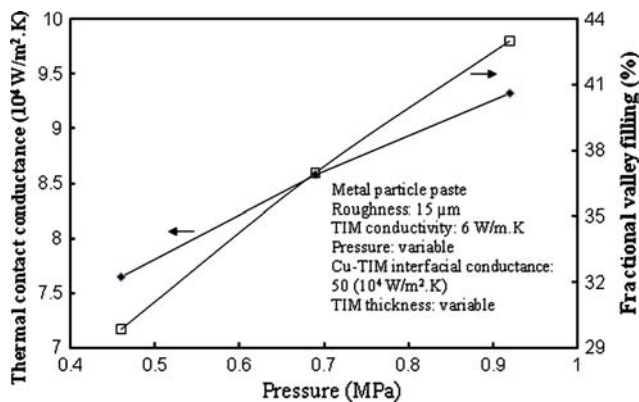


Fig. 25. Effect of pressure on the thermal contact conductance and on the fractional final valley filling for the metal particle paste as the TIM (the rough case).

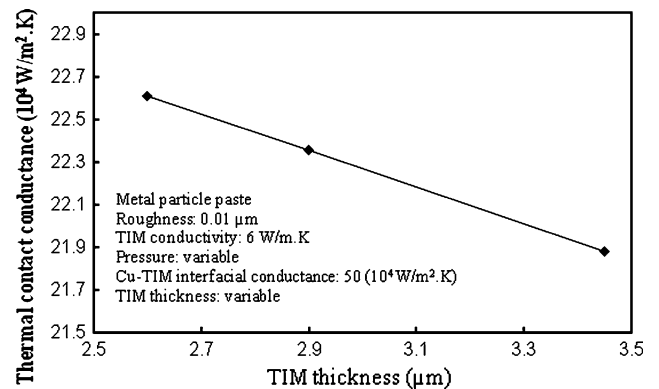


Fig. 28. Effect of the TIM thickness on the thermal contact conductance for the metal particle paste as the TIM (the smooth case).

increasing thickness. That TCC increases with increasing pressure (Fig. 25) is due to a combination of higher fractional valley filling (Fig. 25), larger contact area, and shorter heat flow path.

*Case of smooth copper surfaces:* The effects of (i) the copper-TIM interfacial conductance, (ii) the TIM thermal conductivity, (iii) the TIM thickness, and

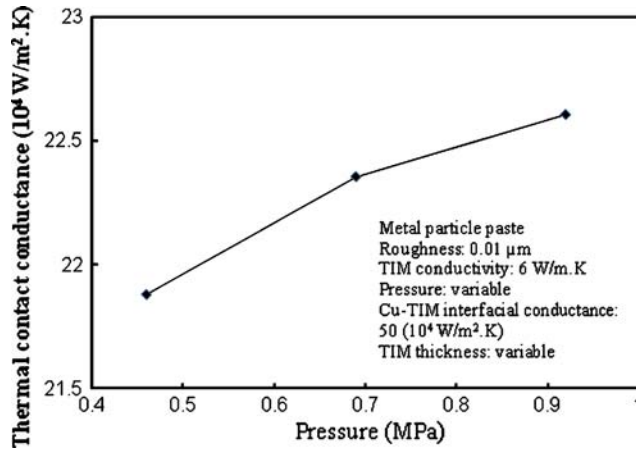


Fig. 29. Effect of pressure on the thermal contact conductance for the metal particle paste as the TIM (the smooth case).

(iv) the pressure on the TCC for the metal particle paste (case of smooth copper blocks) are shown in Figs. 26–29, respectively. The combination of parameters is such that the TCC obtained by the modeling is in line with experimental values.<sup>3,4</sup> The effects are similar to the carbon black paste (case of smooth copper blocks) (Sect. 3.2.1.2). The TCC increases with increasing copper-TIM interfacial conductance (Fig. 26), with TIM thermal conductivity (Fig. 27), with decreasing TIM thickness (Fig. 28), and with increasing pressure (Fig. 29).

#### Extent of the Effect of Each Parameter

The extent of the effect of each parameter on the TCC while all the other parameters are fixed is obtained by calculation of the TCC upon systematic variation of the model parameters. Table II shows the fractional change in TCC per unit fractional change in each parameter, as calculated for both carbon black and metal particle pastes (both rough

and smooth cases for each paste). The fractional change is calculated from the TCC values associated with three values of the relevant parameter that are quite close. One of the three values of the parameter is described in Sect. 3.1, while the other two values are near this value.

In order to obtain more understanding of the effects, additional calculations are conducted for values of each parameter (TIM thickness, TIM thermal conductivity, and TIM-copper interfacial conductance) around the value described in the section “Two-Dimensional Temperature Distribution from Modeling.” Tables III–VI show the results of this additional calculation for each combination of paste type and copper surface roughness. Table VII shows the trends of the effect of each parameter (TIM thickness, TIM thermal conductivity, and TIM-copper interfacial conductance) on the fractional change in TCC per unit fractional change in a parameter (TIM-copper interfacial conductance, TIM thermal conductivity, pressure, copper surface roughness, and TIM thickness) for easier understanding and comparison of the trends shown in Tables III–VI.

Tables III–VII show that, upon increasing the TIM thickness when other parameters are fixed, the effect of the TIM-copper interfacial conductance on TCC decreases and the effect of thermal conductivity on TCC increases. Upon increasing the TIM thermal conductivity when other parameters are fixed, the effect of the TIM-copper interfacial conductance on TCC increases. Upon increasing the TIM-copper interfacial conductance when the other parameters are fixed, the effect of the TIM thermal conductivity on TCC increases.

The results of Tables III–VII are useful for understanding the results in Table II. Table II shows that the TCC is affected by the interfacial conductance much more for the metal particle paste than for the carbon black paste, due to the higher

**Table II. Extent of the Effect of the Various Parameters on the Thermal Contact Conductance (TCC), as Described by the Ratio of the Fractional Change in TCC to the Fractional Change in the Parameter**

Parameter	Ratio (%)			
	Carbon Black Paste		Metal Particle Paste	
	Rough	Smooth	Rough	Smooth
TIM-copper interfacial conductance	43.7 <sup>a</sup>	55.4	85.8	89.1
Copper-copper interfacial conductance	39.0 <sup>a</sup>	0	0	0
TIM thermal conductivity	17.2 <sup>a</sup>	45.2	14.6	11.1
Pressure	42.9 <sup>a</sup>	27.2	29.3	4.9
Copper roughness	-2.1 <sup>a</sup>	0	-10.4	0
TIM thickness	-156 <sup>b</sup>	-45.4	25.0	-11.1

The calculation is performed using the set of parameters chosen for each combination of paste type and copper surface roughness, as described in section “Two-Dimensional Temperature Distribution from Modeling”; <sup>a</sup>Direct contact between two copper hillocks for all of the data points used for calculating this ratio; <sup>b</sup>Direct contact between two copper hillocks for only some of the data points used for calculating this ratio.

**Table III. Extent of the Effect of the Various Parameters on the TCC, as Described by the Ratio of the Fractional Change in TCC to the Fractional Change in a Parameter, as Calculated for the Metal Particle Paste (Case of Rough Copper Surfaces) at Selected Values of the TIM thickness, TIM Thermal Conductivity, and the TIM-Copper Interfacial Conductance**

Parameter	Ratio (%)								
	Thickness ( $\mu\text{m}$ )			Thermal Conductivity (W/m K)			Interfacial Conductance ( $10^4 \text{ W/m}^2 \text{ K}$ )		
	3.5	4.2	5.0	4	6	8	30	50	70
Interfacial conductance	85.8	82.7	80.8	83.5	85.8	88.4	90.6	85.8	80.32
Thermal conductivity	14.6	17.1	19.2	20.1	14.6	10.5	9.7	14.6	19.1
Pressure	29.3	27.0	32.6	29.0	29.3	29.6	29.5	29.3	29.3
Copper roughness	-10.4	-4.5	-7.4	-10.3	-10.4	-10.6	-10.6	-10.4	-10.9
Thickness	19.8	16.9	7.6	19.6	19.8	23.3	30.6	25.0	20.7

**Table IV. Extent of the Effect of the Various Parameters on the TCC, as Described by the Ratio of the Fractional Change in TCC to the Fractional Change in a Parameter, as Calculated for the Carbon Black Paste (Case of Rough Copper Surfaces) at Selected Values of the TIM Thickness, TIM Thermal Conductivity, and the TIM-Copper Interfacial Conductance**

Parameter	Ratio (%)								
	Thickness ( $\mu\text{m}$ )			Thermal Conductivity (W/m K)			Interfacial Conductance ( $10^4 \text{ W/m}^2 \text{ K}$ )		
	0.42	0.75	1.1	0.1	0.128	0.156	90	105	120
Interfacial conductance	43.7 <sup>a</sup>	23.6	18.9	18.9	23.6	27.3	31.5	23.6	21.8
Thermal conductivity	17.2 <sup>a</sup>	74.2	82.9	81.1	74.2	73.6	72.0	74.2	83.8
Pressure	39.8 <sup>a</sup>	31.4	30.1	31.1	31.4	34.6	31.4	31.4	31.6
Copper roughness	-2.0 <sup>a</sup>	-9.0	-10.7	-7.2	-9.0	-7.8	-6.2	-9.0	-8.8
TIM thickness	-87.2 <sup>b</sup>	-530 <sup>b</sup>	-95.3 <sup>a</sup>	-649 <sup>b</sup>	-530 <sup>b</sup>	-451 <sup>b</sup>	-510 <sup>b</sup>	-530 <sup>b</sup>	-553 <sup>b</sup>

<sup>a</sup>Direct contact between two copper hillocks for all of the data points used for calculating this ratio; <sup>b</sup>Direct contact between two copper hillocks for only some of the data points used for calculating this ratio.

**Table V. Extent of the Effect of the Various Parameters on the TCC, as Described by the Ratio of the Fractional Change in TCC to the Fractional Change in a Parameter, as Calculated for the Metal Particle Paste (Case of Smooth Copper Surfaces) at Selected Values of the TIM Thickness, TIM Thermal Conductivity, and the TIM-Copper Interfacial Conductance**

Parameter	Ratio (%)								
	Thickness ( $\mu\text{m}$ )			Thermal Conductivity (W/m K)			Interfacial Conductance ( $10^4 \text{ W/m}^2 \text{ K}$ )		
	2.6	2.9	3.45	4	6	8	30	50	70
Interfacial conductance	90.1	89.1	87.4	84.9	89.1	91.8	93.5	89.1	85.4
Thermal conductivity	10.1	11.1	12.6	15.6	11.1	8.4	7.0	11.1	14.5
Pressure	4.4	4.9	3.6	6.8	4.9	3.8	3.1	4.9	6.5
Thickness	-9.7	-11.1	-13.4	-13.8	-11.1	-7.5	-6.2	-11.1	-13.1

**Table VI. Extent of the Effect of the Various Parameters on the TCC, as Described by the Ratio of the Fractional Change in TCC to the Fractional Change in a Parameter, as Calculated for the Carbon Black Paste (Case of Smooth Copper Surfaces) at Selected Values of the TIM Thickness, TIM Thermal Conductivity, and the TIM-Copper Interfacial Conductance**

Parameter	Ratio (%)								
	Thickness ( $\mu\text{m}$ )			Thermal Conductivity (W/m K)			Interfacial Conductance ( $10^4 \text{ W/m}^2 \text{ K}$ )		
	0.16	0.2	0.24	0.1	0.128	0.156	90	105	120
Interfacial conductance	60.5	55.4	50.3	49.1	55.4	59.9	58.8	55.4	52.1
Thermal conductivity	39.8	45.2	49.6	51.3	45.2	40.2	41.4	45.2	48.7
Pressure	32.2	27.2	19.9	31.1	27.2	24.2	24.8	27.2	29.2
Thickness	-37.7	-45.4	-49.8	-39.1	-45.4	-31.6	-31.6	-45.4	-36.9

**Table VII. How the Value of a Parameter (Thickness, Thermal Conductivity or Interfacial Conductance) Affects the Fractional Change in TCC Per Unit Fractional Change in a Parameter (TIM-Copper Interfacial Conductance, TIM Thermal Conductivity, Pressure, Copper Surface Roughness, and TIM Thickness)**

Parameter	Thickness ( $\mu\text{m}$ )				Thermal Conductivity (W/m K)				Interfacial Conductance ( $10^4 \text{ W/m}^2 \text{ K}$ )			
	Carbon Black Paste		Metal Particle Paste		Carbon Black Paste		Metal Particle Paste		Carbon Black Paste		Metal Particle Paste	
	R	S	R	S	R	S	R	S	R	S	R	S
Interfacial conductance	-	-	-	-	+	+	+	+	-	-	-	-
Thermal conductivity	+	+	+	+	-	-	-	-	+	+	+	+
Pressure	-	-	~	~	+	-	+	-	~	~	+	+
Copper roughness	+	0	~	0	~	0	+	0	~	0	~	0
Thickness	~	+	-	+	-	~	+	-	+	~	-	+

The trends are based on the results in Tables III–VI; +: Increasing the value of the parameter above will increase the fractional change in TCC per unit fractional change in the parameter to the left; -: Increasing the value of the parameter above will decrease the fractional change in TCC per unit fractional change in the parameter to the left; ~: No trend for how the value of parameter above affects the fractional change in TCC per unit fractional change in the parameter to the left; 0: No effect of the value of parameter above on the fractional change in TCC per unit fractional change in the parameter to the left; R: rough copper surfaces; S: smooth copper surfaces.

thermal conductivity and lower interfacial conductance of the metal particle paste compared with the carbon black paste; both an increase in the thermal conductivity and a decrease in the interfacial conductance increase the effect of the interfacial conductance (Tables III–VII).

Table II shows that the TCC is affected by pressure more for the carbon black paste than for the metal particle paste, whether the copper surfaces are rough or smooth. In the smooth case, this is due to the higher thermal conductivity and lower interfacial conductance of the metal particle paste (Tables V–VII). In the rough case, this is due to the direct contact between the two copper blocks when the carbon black paste is the TIM with a very low thickness.

Although increasing the thickness increases the effect of thermal conductivity (Tables III–VII), carbon black paste with a lower thickness is more

affected by thermal conductivity than is the metal particle paste with a higher thickness (Table II). This is a result of the high interfacial conductance and the low thermal conductivity of the carbon black paste, as both a high interfacial conductance and a low thermal conductivity increase the effect of the thermal conductivity on TCC (Tables III–VII). The strong effect of the TIM thickness on the carbon black paste in the rough case is because of the direct contact of copper blocks, which disappears with increasing thickness.

The last row of Table II shows a different sign for the effect of TIM thickness for the metal particle paste (rough copper surfaces) compared with that for the other three cases. A positive sign of the fractional change in TCC per unit fractional change in the thickness (e.g., TCC increasing with increasing thickness) is because increasing the metal particle paste thickness increases both the

heat flow path and the fractional valley filling. In this range of thickness, the positive effect of increasing the fractional valley filling is dominant and causes TCC to increase. On the other hand, in the case of smooth copper surfaces (100% fractional valley filling) or in the case of rough copper surfaces with carbon black as the TIM (with very low thickness), increasing the thickness makes the heat flow path longer and consequently decreases the TCC.

As shown in Table II, for the carbon black paste, the TCC is most affected by the thickness in the rough case and by the interfacial conductance in the smooth case. For the metal particle paste, the TCC is most affected by the interfacial conductance in both the rough and smooth cases.

### Comparison of Modeling and Experimental Results

Table VIII shows the fractional valley filling, as obtained from the modeling results. In the smooth case, the fractional valley filling of both the carbon black paste and the metal particle paste is 100% because the hillock height is  $0.01 \mu\text{m}$ , which is negligible compared to the TIM thicknesses ( $0.16 \mu\text{m}$  to  $3.4 \mu\text{m}$ ). In the rough case, the fractional valley filling is less than 100%, thus allowing the change in TCC to be related to the change of the fractional valley filling (see the sections “Effects of Various Parameters on the Calculated Thermal Contact Conductance” and “Extent of the Effect of Each Parameter”). In particular, for the carbon black paste in the rough case, the fractional valley filling is 6% and is independent of the pressure. The pressure independence is because the TIM thickness is independent of the pressure—a consequence of the direct contact between the copper surfaces. For the metal particle paste in the rough case, the fractional valley filling ranges from 30% to 43%, such that the value increases with decreasing TIM thickness. This trend is because, with increasing pressure, two copper hillocks become closer and the

paste occupies more of the valley. The TIM thickness decreases when the copper hillocks become closer and the fractional valley filling increases when the paste enters the valley.

Table VIII shows good agreement between modeling and experiment for the carbon black paste and the metal particle paste in both smooth and rough cases. The agreement between modeling and experiment is better for the metal particle paste than for the carbon black paste. This is because of the greater difficulty in modeling the carbon black paste, due to the involvement of both the TIM-copper interface and the copper-copper interface.

In the rough case, as a result of the small thickness of the carbon black paste ( $0.4 \mu\text{m}$ ) compared with the metal particle paste ( $2.9 \mu\text{m}$  to  $4.0 \mu\text{m}$ ), the TIM-copper contact area and fractional valley filling of the carbon black paste are smaller than those for the metal particle paste. However, the TCC is higher for the carbon black paste due to the direct contact between the copper blocks and the high copper-copper interfacial conductance.

In the smooth case, the carbon black paste gives a higher TCC than the metal particle paste. This is because of the low modulus and the small thickness of the carbon black paste. The small thickness decreases the heat flow path length between the two copper surfaces and consequently increases the TCC.

### CONCLUSION

This paper uses finite element modeling to evaluate the relative importance of the factors that govern the performance of thermal pastes. The modeling involves heat flow across the thermal contact and provides the two-dimensional temperature distribution. The thermal contact in the initial state is modeled as one semicircular hillock for each of the two proximate surfaces, such that the bottom of the semicircle in the upper surface is vertically in line with the top of the semicircle in the lower surface.

**Table VIII. Thermal Contact Conductance (TCC), Bond-Line Thickness, and Fractional Valley Filling for Various Combinations of Thermal Paste Type and Copper Surface Roughness**

Thermal Paste	Roughness ( $\mu\text{m}$ )	Pressure (MPa)	TCC ( $10^4 \text{ W/m}^2 \text{ K}$ ) <sup>a</sup>	TCC ( $10^4 \text{ W/m}^2 \text{ K}$ ) <sup>b</sup>	Bond-Line Thickness ( $\mu\text{m}$ )	Fractional Valley Filling (%) <sup>b</sup>
Metal particle	15	0.46	$7.76 \pm 0.14$	6.31	$4.0^c$	29.9
Metal particle	15	0.69	$8.43 \pm 0.20$	7.27	$3.3^c$	37.0
Metal particle	15	0.92	$8.78 \pm 0.11$	7.45	$2.9^c$	43.0
Carbon black	15	0.46	$8.72 \pm 0.11$	6.67	$0.4^d$	6.1
Carbon black	15	0.69	$10.18 \pm 0.11$	7.87	$0.4^d$	6.1
Carbon black	15	0.92	$11.12 \pm 0.27$	9.07	$0.4^d$	6.1
Metal particle	0.01	0.46	$19.87 \pm 0.27$	21.87	$3.4^c$	100
Metal particle	0.01	0.69	$22.55 \pm 0.43$	22.35	$2.9^c$	100
Carbon black	0.01	0.46	$25.91 \pm 0.16$	29.31	$0.24^d$	100
Carbon black	0.01	0.69	$27.75 \pm 0.14$	32.26	$0.20^d$	100

<sup>a</sup>Experimental results<sup>3-5</sup>; <sup>b</sup>Modeling results; <sup>c</sup>Experimental results<sup>25</sup>; <sup>d</sup>Experimental results.<sup>4,5</sup>

A paste of a controlled initial thickness is sandwiched at a controlled pressure by copper surfaces with a controlled initial roughness. The effects of the conductance of the interface between the paste and copper and that of the interface between the two copper surfaces, the thermal conductivity of the paste, the pressure, and the copper roughness on the thermal contact conductance of the sandwich and on the fractional valley filling by the pastes are thus quantified for both the carbon black paste and the metal particle paste. The effects of pressure, paste thickness, and copper surface roughness on performance are mainly due to the change in the fractional filling of the valleys in the copper surface topography in most cases. Due to the low solid content, the carbon black paste is much lower in modulus than the metal particle paste, and the paste thickness is much smaller for the former. The performance of the carbon black paste is most affected by the thickness in the rough case and by the paste-copper interfacial conductance in the smooth case, whereas that of the metal particle paste is most affected by the paste-copper interfacial conductance. Good agreement is found between modeling and experimental results.

#### ACKNOWLEDGEMENT

Experimental data from Mr. Chuangang Lin, University at Buffalo, State University of New York, are much appreciated.

#### REFERENCES

1. D.D.L. Chung, *Adv. Microelectron.* 33, 8 (2006).
2. R. Prasher, *Proc. IEEE* 94, 1571 (2006). doi:10.1109/JPROC.2006.879796.
3. C. Lin and D.D.L. Chung, *J. Mater. Sci.* 42, 9245 (2007). doi:10.1007/s10853-007-1911-4.
4. C. Lin and D.D.L. Chung, *SAMPE Tech. Conf. Proc.* (2008) Accepted.
5. C. Lin and D.D.L. Chung, *Carbon* (in press).
6. C.-K. Leong and D.D.L. Chung, *Carbon* 41, 2459 (2003). doi:10.1016/S0008-6223(03)00247-1.
7. C.-K. Leong and D.D.L. Chung, *Carbon* 42, 2323 (2004). doi:10.1016/j.carbon.2004.05.013.
8. C.-K. Leong, Y. Aoyagi, and D.D.L. Chung, *J. Electron. Mater.* 34, 1336 (2005). doi:10.1007/s11664-005-0259-2.
9. C.-K. Leong, Y. Aoyagi, and D.D.L. Chung, *Carbon* 44, 435 (2006). doi:10.1016/j.carbon.2005.09.002.
10. A. Timothy, T.A. Howe, C.-K. Leong, and D.D.L. Chung, *J. Electron. Mater.* 35, 1628 (2006). doi:10.1007/s11664-006-0209-7.
11. C. Lin, T.A. Howe, and D.D.L. Chung, *J. Electron. Mater.* 36, 659 (2007). doi:10.1007/s11664-007-0116-6.
12. Y. Xu, C.-K. Leong, and D.D.L. Chung, *J. Electron. Mater.* 36, 1181 (2007). doi:10.1007/s11664-007-0188-3.
13. T. Lee, K. Chiou, F. Tseng, and C. Huang, *Proc. 55th Electronic Components and Tech. Conf.*, Vol. 1 (Piscataway, NJ, IEEE, 2005), pp. 55–59.
14. J.L. Sample, K.J. Rebello, H. Saffarian, and R. Osiander, *9th Intersociety Conf. on Thermal and Thermomechanical Phenomena in Elec. Sys.*, Vol. 1 (Piscataway, NJ, IEEE, 2004), pp. 297–301.
15. H.F. Chuang, S.M. Cooper, M. Meyyappan, and B.A. Cruden, *J. Nanosci. Nanotechnol.* 4, 964 (2004). doi:10.1166/jnn.2004.152.
16. Q. Ngo, B.A. Cruden, A.M. Cassell, G. Sims, M. Meyyappan, J. Li, and C.Y. Yang, *Nano Lett.* 4, 2403 (2004). doi:10.1021/nl048506t.
17. Y. Wu, C.H. Liu, H. Huang, and S.S. Fan, *Appl. Phys. Lett.* 87, 213108-1 (2005).
18. E.E. Marotta, S.J. Mazzuca, and J. Norley, *IEEE Trans. Compon. Packag. Tech.* 28, 102 (2005). doi:10.1109/TCAPT.2004.843153.
19. S. Shaikh, K. Lafdi, and E. Silverman, *Carbon* 45, 695 (2007). doi:10.1016/j.carbon.2006.12.007.
20. C.-P. Chiu, G.L. Solbrekken, and Y.D. Chung, *13th IEEE Semiconductor Thermal Management and Management Symp.*, Institute of Electrical and Electronics Engineers, Vol. 57 (1997).
21. R.A. Shaik, A.N. Beall, and A. Razani, *Heat Transf. Eng.* 22, 41 (2001). doi:10.1080/01457630150215712.
22. M.G. Cooper, B.B. Mike, and M.M. Yovanovich, *Int. J. Heat Mass Trans.* 12, 279 (1969). doi:10.1016/0017-9310(69)90011-8.
23. J.A. Greenwood and J.B.P. Williamson, *Proc. R. Soc. Lond. A Math. Phys. Sci.* 295, 300 (1966). doi:10.1098/rspa.1966.0242.
24. N.B. Vargaftik, *Handbook of Thermal Conductivity of Liquids and Gases* (Boca Raton: CRC, 1994).
25. C. Lin and D.D.L. Chung, unpublished results.